Synthesis, Structure and Physical Properties of Tetrabutylammonium Salts of Nickel Complexes with the New Ligand dcbdt = 4,5-dicyanobenzene-1,2-dithiolate, $[Ni(dcbdt)_2]^{z-}$ (z = 0.4, 1, 2)

Dulce Simão,[a] Helena Alves,[b] Dulce Belo,[b] Sandra Rabaça,[b] Elsa Branco Lopes,[b] Isabel Cordeiro Santos,[b] Vasco Gama,[b] Maria Teresa Duarte,[a] Rui Teives Henriques,[a,b] Horácio Novais,[a] and Manuel Almeida*[b]

Keywords: S ligands / Charge transfer / Nickel / Cyclic voltammetry / Magnetic properties

The synthesis and characterization of the new aromatic *ortho*-dithiol, 4,5-dicyanobenzene-1,2-dithiol (**3**) is reported. This compound was used to prepare tetrabutylammonium salts of novel nickel complexes; the nickel(II) salt $(n\mathrm{Bu_4N})_2[Ni(dcbdt)_2]$ (**4**), the nickel(III) salt $(n\mathrm{Bu_4N})_2[Ni(dcbdt)_2]_2$ (**5**), and the partially oxidized $Ni^{III/IV}$ salt $(n\mathrm{Bu_4N})_2[Ni(dcbdt)_2]_5$ (**6**). (dcbdt = 4,5-dicyanobenzene-1,2-dithiolate). The Ni^{II} complex presents a square-planar coordination geometry and is diamagnetic, while in the paramagnetic Ni^{III} complex the $Ni(dcbdt)_2$ units are strongly dimerized with the metal atom in a square-pyramidal coordination geometry and its magnetic susceptibility follows a singlet-triplet model with an antiferromagnetic coupling J = 897 K. The partially oxidized $Ni^{III/IV}$ complex **6** presents a weakly temperature-dependent paramagnetism of $5–6\cdot10^{-4}$ emu/mol and a room-temperature electrical conductivity of 0.15 S/cm following a semiconducting regime.

Introduction

Bis(dithiolene) transition metal complexes, showing a variety of coordination geometries and oxidation states, have been extensively studied since the 1960s,[1] and they have been widely used as building blocks for molecular compounds with conducting and or magnetic properties.[2] Among the simple examples of such complexes are the $M(mnt)_2$ complexes based on the ligand mnt = 1,2-dicyanoethene-1,2-dithiolate, also known as maleonitriledithiolate (Scheme 1), first prepared in 1955 by Bähr and Schleitzer.[3] These simple $M(mnt)_2$ complexes have provided the basis of compounds with very interesting properties such as metallic conductivity,[4] magnetic chains in compounds also having conducting chains based on other donor species,[5] and even ferroelectric behaviour.[6] However, it is believed that more extended and delocalized π-ligands of this type would make the different oxidation states more accessible, favouring electron transport in the solid, and offering a richer variety of structures. Indeed, other bis(dithiolene) complexes with delocalized sulfur-rich ligands have provided the bases for many other metallic and even superconducting systems.[2]

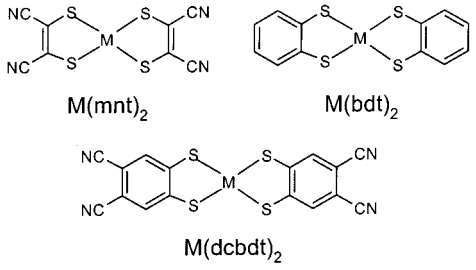

Scheme 1

In order to explore chemical modifications on electron charge-transfer solids containing the $M(mnt)_2$ complexes, we decided to prepare analogous dicyanodithio complexes with the more extended and aromatic ligand 4,5-dicyanobenzene-1,2-dithiol (**3**), (H_2dcbdt), whose preparation was not previously described. Preliminary data on a gold complex with this ligand, $(n\mathrm{Bu_4N})_2[Au(dcbdt)_2]_5$, was recently reported by us.[7] In this paper we report the synthesis of the ligand and the preparation and characterization of the tetrabutylammonium salts of three different nickel complexes, $[Ni(dcbdt)_2]^{z-}$ (z = 0.4, 1, 2).

Results and Discussion

The key compound for the synthesis of the ligand is 4,5-dichloro-1,2-dicyanobenzene (**1**) that can be obtained from 4,5-dichlorophthalic anhydride,[8] and is actually commercially available. The followed synthetic procedure involved the preparation of the aromatic dibenzyl sulfide,[9] 1,2-bis(*S*-benzylthio)-4,5-dicyanobenzene (**2**), in 71% yield (m.p. 189–190 °C), followed by a mild cleavage with the assistance of anhydrous aluminium chloride[10] (Scheme 2) to obtain **3** in 53% yield [m.p. 100 °C (dec.)].

[a] Departamento de Engenharia Química,
Instituto Superior Técnico
Av. Rovisco Pais, 1049-001 Lisboa, Portugal
Fax: (internat.) + 351-218490844
E-mail: dulce@alfa.ist.utl.pt
[b] Departamento de Química, Instituto Tecnológico Nuclear
Estrada Nacional no. 10, 2685-953 Sacavém, Portugal
Fax: (internat.) + 351-219941455
E-mail: malmeida@itn.pt

  1434–1948/01/1212–3119 $ 17.50+.50/0

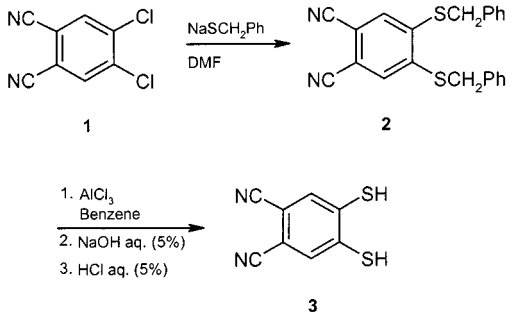

Scheme 2

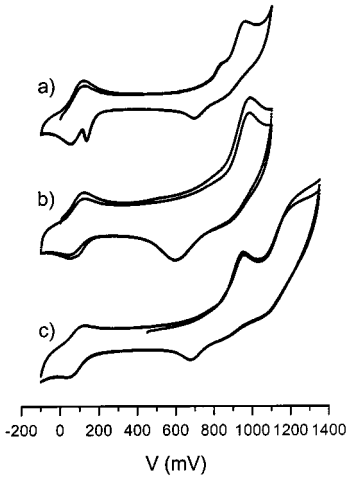

Figure 1. Cyclic voltammograms of $(n\mathrm{Bu_4N})_2[\mathrm{Ni(dcbdt)_2}]_2$ (**5**) in acetonitrile solution (ref. $Ag/AgNO_3$) at different scan rates: a) 50 mV/s; b) 500 mV/s; c) 100 mV/s

The nickel(II) complex of the ligand 4,5-dicyanobenzene-1,2-dithiol was obtained by the reaction of the dithiolate with nickel chloride, in an aqueous/alcoholic solvent mixture, and precipitated in the form of the tetrabutylammonium salt $(n\mathrm{Bu_4N})_2[\mathrm{Ni(dcbdt)_2}]$ (**4**) (Scheme 3), following the usual procedure for other bis(dithiolene) complexes.[11] This complex could be oxidized to Ni^{III}, $(n\mathrm{Bu_4N})_2[\mathrm{Ni(dcbdt)_2}]_2$ (**5**), with iodine in acetone solutions (yield 44%, m.p. 244−245 °C). Further electrochemical oxidation of **5** led to a mixed Ni^{III}/Ni^{IV} compound $(n\mathrm{Bu_4N})_2[\mathrm{Ni(dcbdt)_2}]_5$ (**6**).

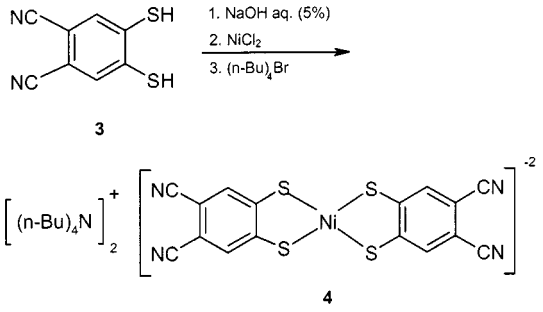

Scheme 3

The cyclic voltammetry of $(n\mathrm{Bu_4N})_2[\mathrm{Ni(dcbdt)_2}]_2$ (**5**) in acetonitrile showed different redox processes (Figure 1). One pair of reversible waves at 0.08 V vs. $Ag/AgNO_3$ was always present, as in $(n\mathrm{Bu_4N})_2[\mathrm{Ni(dcbdt)_2}]$ (**4**), and it was ascribed to the couple Ni^{II}/Ni^{III}. This value should be compared with the corresponding one for the compound with the unsubstituted benzodithiolate ligand (bdt), $Ni(bdt)_2$ (−1.05 V),[12] showing that the two cyano groups stabilize the dianionic state. In fact, while the $Ni(bdt)_2^-$ complex was obtained by oxidation of the dianion in air, obtaining $Ni(dcbdt)_2^-$ from the dianion required iodine as the oxidizing agent.

At more positive potentials a series of irreversible waves were observed with oxidation peaks at 0.83, 0.94, and 1.2 V, and reductions at 1.08, 0.89, and 0.68 V. The first oxidation wave became less prominent at higher scan rates (above 100 mV/s), while the corresponding reduction wave changed position from 0.70 to 0.50 V as the rate increased from 50 to 3000 mV/s. For slow scanning rates (50−100 mV/s) with amplitudes above 0.9 and below 1.2 V, there was an additional reduction peak at 0.120 V, typical of the formation upon oxidation of adsorbed species on the electrode (Figure 1, a). This peak was no longer observed at a scan rate of 500 mV/s and above (Figure 1, b) or for sweeps of 1.2 V or above (Figure 1, c).

This suggests that the process at 0.94/0.89 V led to the formation of insoluble $[\mathrm{Ni(dcbdt)_2}]_5^{2-}$ at the electrode. In fact from dichloromethane solutions of the monoanionic complex $(n\mathrm{Bu_4N})_2[\mathrm{Ni(dcbdt)_2}]_2$ (**5**), crystals of $(n\mathrm{Bu_4N})_2[\mathrm{Ni(dcbdt)_2}]_5$ (**6**) were obtained by electrocrystallization, using similar conditions to those previously described to obtain the gold analogue.[7] The higher potential process is probably the full oxidation to Ni^{IV}, while the waves at 0.83/0.68 with a very rate-sensitive reduction peak were associated with the process $[\mathrm{Ni(dcbdt)_2}]_2^{-2}/[\mathrm{Ni(dcbdt)_2}]_2^-$, coupled to some other reaction.

The direct comparison of this with cyclic voltammetry data obtained with $(n\mathrm{Bu_4N})_2[\mathrm{Ni(dcbdt)_2}]$ (**4**) was not possible due to the much lower solubility of compound **4**. The results for compound **4** present the same pair of reversible waves at 0.086 V, and the two similar pairs of waves at higher oxidation potentials. However, the waves at 0.83/ca. 0.68 V and the reduction wave ascribed to electrode deposition were not observed. This may be due only the lower solubility of **4**.

Compound **5** probably exists in solution as the dimer $[\mathrm{Ni(dcbdt)_2}]_2^{2-}$ as suggested by the solid-state X-ray structure with quite short dimerization bonds (see below). This

proposal is also supported by the comparison of the conductivity of **4** and **5** in acetonitrile solutions. If compound **5** were fully dissociated, the conductivity of an equimolar solution of **4** should have been twice that of **5**, but we found values of 57.5 and 22.7 μS/cm, respectively, for 0.2 mM solutions at 18 °C, giving a higher ratio and denoting the presence of the less mobile dimer.

The crystals obtained for compounds **4** and **5** enabled the crystal-structure determination by X-ray diffraction, but those of **6** were of insufficient quality for diffraction work. An ORTEP view of the complex anions in **4** and **5** is depicted in Figure 2, showing the atomic labelling scheme. Selected bond lengths for these compounds are presented in Table 1.

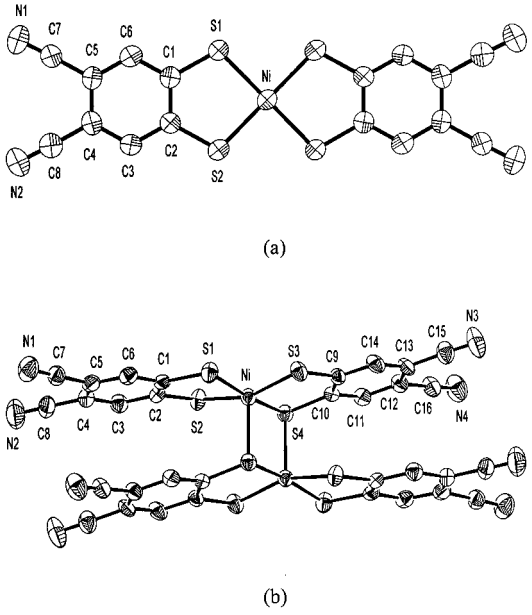

Figure 2. ORTEP diagrams and atomic numbering scheme of the complexes; a) $[Ni(dcbdt)_2]^{2-}$ in **4** and b) $[Ni(dcbdt)_2]^{-}$ in **5**, with thermal ellipsoids at 40% probability level

In complex **4** the Ni atom is located at an inversion centre, and the dianion $[Ni(dcbdt)_2]^{2-}$ presents a perfectly planar geometry, since all atoms lie in a mirror plane. The Ni−S bond lengths, Ni−S(2) 2.1736(15) Å and Ni−S(1) 2.1658(16) Å, are in the typical range, 2.16−2.18 Å, of other bis(dithio)Ni^{II} complexes,[13−16] namely for $Ni(bdt)_2$ where the distances are 2.166−2.172 Å.[16] The crystal structure of **4** shows $[Ni(dcbdt)_2]^{2-}$ layers with the complex in mirror planes at $y = 0$ and $y = 1/2$, which are separated by cation layers (Figure 3) preventing any short anion−anion interactions.

In **5** the Ni^{III} complex presents a strong dimerization of the $[Ni(dcbdt)_2]^{-}$ units that are related by an inversion centre (Figure 2) between the two nickel atoms. In the $[Ni(dcbdt)_2]_2^{2-}$ units, besides the equatorial Ni−S bonds at distances Ni−S(1) 2.2050(17) Å, Ni−S(2) 2.2023(16) Å, Ni−S(3) 2.1993(16) Å, Ni−S(4) 2.1792(16) Å, there are two Ni−S(4)* bonds at 2.3965(16) Å.

As shown by the side view of the dimer $[Ni(dcbdt)_2]_2^{2-}$ in Figure 4, the ligand where one sulfur atom is coordinating two metal atoms is almost planar [the largest deviations being the S(3) 0.072 Å and S(4) 0.083 Å] and the Ni atom lies only 0.08 Å from its average plane. In contrast, the other ligand presents a more considerable distortion with the coordinating sulfur atoms S1 and S2 deviated in opposite directions (0.063 and −0.127, respectively) and the Ni atom −0.39 Å from its average plane. Thus the four coordinating sulfur atoms are not coplanar and present a significant tetrahedral distortion with deviations of ±0.137 Å from their average plane, while the Ni atom deviates 0.286 Å from the average plane of the four sulfur atoms. The average plane of the two ligands makes a dihedral angle of 9.39(17)°.

Table 1. Selected bond lengths [Å] for $[Ni(dcbdt)_2]$ complexes

	$[Ni(dcbdt)_2]^{2-}$	$[Ni(dcbdt)_2]_2^{2-}$
Ni−S(1)	2.1658(16)	2.2050(17)
Ni−S(2)	2.1736(15)	2.2023(16)
Ni−S(3)		2.1993(16)
Ni−S(4)		2.1792(16)
Ni−S(4)[a]		2.3965(16)
S(1)−C(1)	1.729(6)	1.738(5)
S(2)−C(2)	1.725(6)	1.732(5)
S(3)−C(9)		1.734(5)
S(4)−C(10)		1.752(5)
C(1)−C(6)	1.384(7)	1.409(7)
C(1)−C(2)	1.424(8)	1.414(7)
C(2)−C(3)	1.394(7)	1.398(7)
C(6)−C(5)	1.388(7)	1.380(7)
C(3)−C(4)	1.389(7)	1.377(7)
C(5)−C(4)	1.403(8)	1.401(7)
C(5)−C(7)	1.436(8)	1.450(7)
C(4)−C(8)	1.441(8)	1.448(8)
C(7)−N(1)	1.144(7)	1.134(7)
C(8)−N(2)	1.135(6)	1.130(7)
C(9)−C(14)		1.394(7)
C(9)−C(10)		1.406(7)
C(10)−C(11)		1.376(6)
C(14)−C(13)		1.385(7)
C(11)−C(12)		1.374(7)
C(13)−C(12)		1.411(7)
C(13)−C(15)		1.447(8)
C(12)−C(16)		1.444(7)
C(15)−N(3)		1.125(7)
C(16)−N(4)		1.131(7)

[a] $-x,-y,-z+1$.

The dimerization of bis(dithiolene)metal(III) complexes, with the metal atom presenting a square-pyramidal coordination geometry, is frequent in similar complexes of other metals such as Fe and Co.[1,17,18] For bis(dichalcogenato)-nickel complexes such a clear dimeric structure was only found in a few bis(diselenolato)Ni complexes, as the neutral $Ni^{IV}(ddds)_2$ complex (ddds = 5,6-dihydro-1,4-dithiin-2,3-diselenolate),[19] the partially oxidised $Me_4N[Ni(dsise)_2]_2^{+}$ (dsise = 1,3-dithio-2-selenenido-4,5-diselenolate),[20] and the Ni^{III} complex $nBu_4N[Ni(dsit)_2]$ (dsit = 1,3-dithiole-2-thione-4,5-diselenolate).[21] With complex $Ni(mnt)_2^{-}$ a much weaker tendency towards a metal-over-sulfur packing has been reported in the compounds $(pet)_3[Ni(mnt)_2]_2$,[22] $(PPh_3Me)[Ni(mnt)_2]$,[23] and $NEt_4[Ni(mnt)_2]$,[24] where the

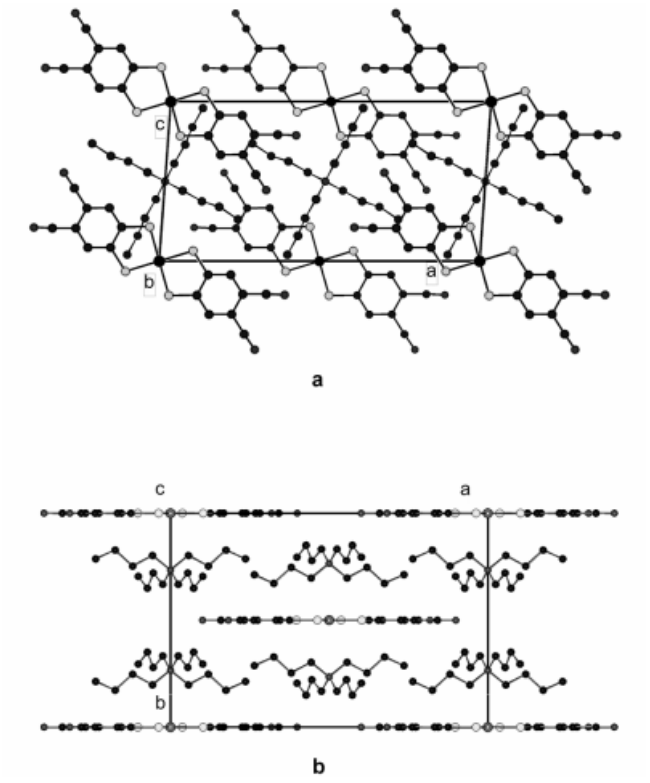

Figure 3. Crystal structure of $(n\mathrm{Bu_4N})_2\mathrm{Ni(dcbdt)_2}$ (**4**): (a) viewed along the *b* axis, and (b) viewed along the *c* axis

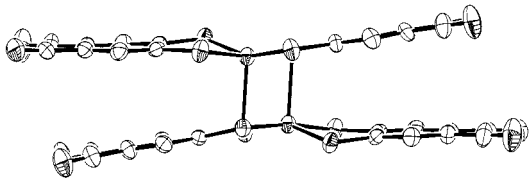

Figure 4. Side view of the dimer $[\mathrm{Ni(dcbdt)_2}^-]_2$ in **5**

apical Ni−S distances are much larger, 3.85, 3.59, and 3.69 Å, respectively, and the $\mathrm{Ni(mnt)_2}$ units remain almost planar. To the best of our knowledge, this is the first time that a clearly dimerized structure was found in a bis(dithio)$\mathrm{Ni^{III}}$ complex. Furthermore, it should be noticed that in this case, when compared with other dimerized bis(dichalcogenide) complexes, the apical bond is quite short and almost comparable to the equatorial ones.

The crystal structure of **5** is shown in Figure 5. Along the axes *c* and *b* the dimerized anions and the cations are alternating. However, along *a* the $[\mathrm{Ni(dcbdt)_2}]_2^{2-}$ dimers are arranged in chains, due to several weak interactions, connecting two $[\mathrm{Ni(dcbdt)_2}]^-$ units of adjacent dimers side by side, namely the hydrogen bonds N(3)···H(3*) and N(3*)···H(3) at 2.612 Å and 156.6°, and S(1)···H(11) at 3.188 Å and 149.9°, and a short contact S(3)···S(3*) at 3.784 Å, (see Figure 6).

While the dianionic complex **4** is diamagnetic, the monoanionic complex **5**, with $\mathrm{Ni^{III}}$, is expected to be paramagnetic with $S = {}^1/_2$. However, the strong dimerization

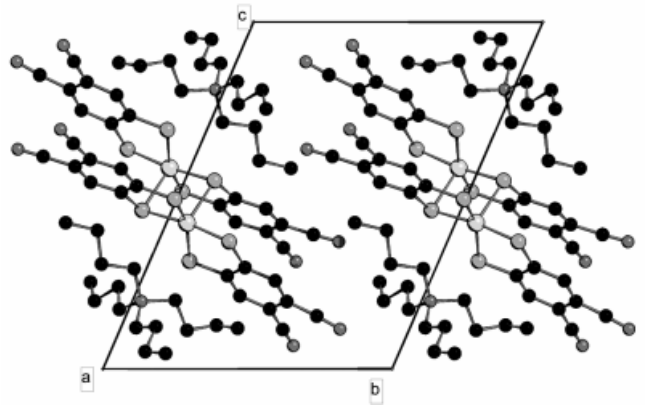

Figure 5. Crystal structure of $(n\mathrm{Bu_4N})_2[\mathrm{Ni(dcbdt)_2}]_2$ (**5**) viewed along the *a* axis

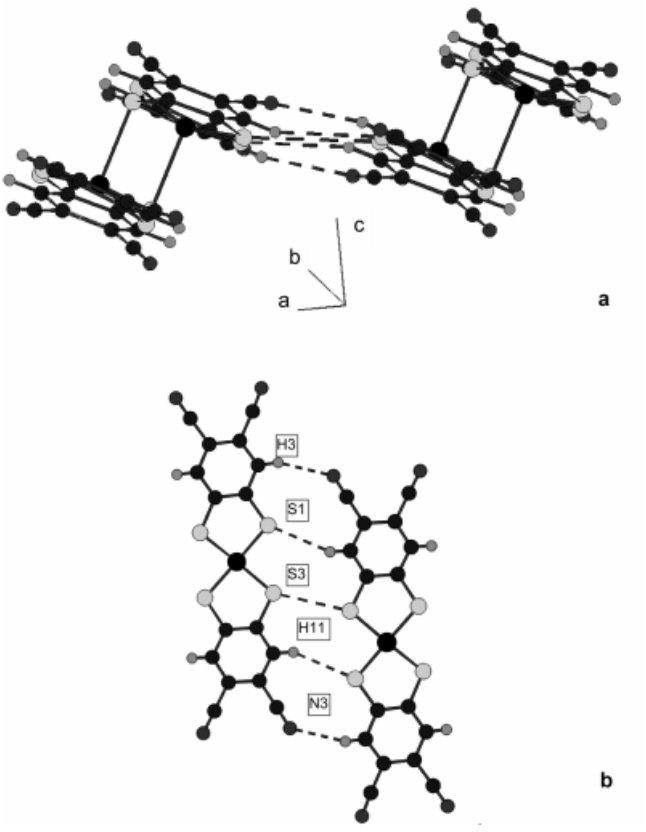

Figure 6. Chain of $[\mathrm{Ni(dcbdt)_2}^-]_2$ dimers in **5** connected along *a* by S···S contacts and N···H and S···H hydrogen bonds: a) side view; b) detail of two $[\mathrm{Ni(dcbdt)_2}]^-$ units of adjacent dimers viewed perpendicularly to their average plane with indication of the short contacts connecting them

of the $[\mathrm{Ni(dcbdt)_2}]^-$ units, as frequently observed in other dimerized Fe complexes, can lead to a strong antiferromagnetic coupling of the $S = {}^1/_2$ states expected for a isolated square planar coordination.[17,22,25]

The EPR spectra of **5**, both as a powder or as a frozen solution, show rhombic symmetry, with *g* values of 2.210, 2.0421, and 2.0064, for acetone solution at 110 K.

$(n\mathrm{Bu_4N})_2[\mathrm{Ni(dcbdt)_2}]_5^{-2}$ also shows an EPR signal, as expected for a partially oxidized $Ni^{III/IV}$ compound, but this signal is visible only at low temperature, as an almost isotropic broad signal, 300G wide and centred at $g = 2.025$ at 8 K.

The paramagnetic susceptibility of $(n\mathrm{Bu_4N})_2[\mathrm{Ni(dcbdt)_2}]_2$, obtained from raw data after a correction for diamagnetism estimated from tabulated Pascal constants as $4.2\cdot10^{-4}$ emu/mol, was ca. $5\cdot10^{-4}$ emu/mol at room temperature and showed a strong decrease upon cooling, reaching a minimum around 100 K (Figure 7). At lower temperatures the magnetic susceptibility became dominated by a Curie tail of impurities and increased again. The paramagnetic susceptibility data could be accurately fitted by a model, considering in addition to the Curie tail and a temperature-independent term a contribution due to the dimers of $S = {}^1/_2$ spins, following a singlet-triplet law as given by the Bleaney−Jones equation.[26]

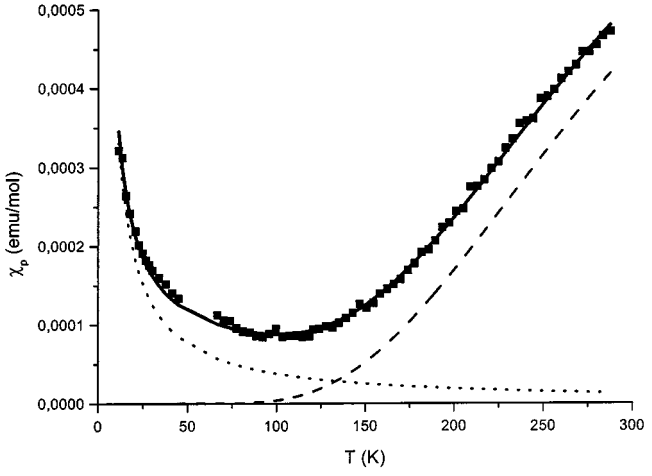

Figure 7. Paramagnetic susceptibility χ_p of $(n\mathrm{Bu_4N})_2[\mathrm{Ni(dcbdt)_2}]_2$ (**5**) as a function of the temperature T: the continuos line is a fit by Equation (1), the dotted line being the Curie tail contribution, corresponding to ca. 0.9% of $S = {}^1/_2$ spins and the dashed line the singlet-triplet contribution of the dimers (see text)

$$\chi_P = A + C/T + (Ng^2\mu_B^2/k_BT)[\exp(-2J/k_BT) + 3]^{-1} \quad (1)$$

with $A = 50(2)\cdot10^{-6}$ emu/mol, $J = 447(4)$ K, $g = 2.79(4)$, and $C = 0.00339(5)$ emu/mol·K corresponding to approximately 0.90% of $S = {}^1/_2$ spins (see Figure 7).

As it can be seen in Figure 7, the fit to our data is very good, but it is worth noting that the g value obtained is too high compared with known isolated Ni^{III} complex, and is above the EPR value obtained for this compound. However, the EPR signal that was visible only at low temperature, where the contribution was negligible, was due to the isolated Ni^{III} species associated with the Curie tail, rather than with the triplet state for which there are no EPR data in dimers of Ni^{III} species.

The J value obtained is quite large and can be compared to those reported for other $Ni(mnt)_2^-$ compounds such as $Cs[Ni(mnt)_2]\cdot H_2O$,[4c] $(pet)_3[Ni(mnt)_2]_2$,[22] $(PPh_3Me)[Ni(mnt)_2]$,[27] and $NEt_4[Ni(mnt)_2]$,[27] where the susceptibility data were also fitted to a similar singlet-triplet model with J values of 197, 226, 352, and 446 K, respectively. It is worth noting that the g values obtained by the fit in the last three compounds are also significantly larger than typical ones for similar isolated Ni^{III} complexes.

The paramagnetic susceptibility of **6**, obtained after a correction for diamagnetism, estimated from tabulated Pascal constants as $6.8\cdot10^{-4}$ emu/mol, is ca. $7\cdot10^{-4}$ emu/mol at room temperature and shows an almost temperature-independent behaviour down to ca. 70 K (Figure 8). Below this temperature there is an increase of susceptibility upon cooling that is ascribed to a Curie tail of impurities (or most likely defects). As shown in Figure 8, this Curie tail is relatively large and corresponds to ca. 5.6% $S = {}^1/_2$ spins. Subtracting this Curie tail from our experimental data an intrinsic susceptibility contribution was obtained that remained almost constant at least above 20 K with values in the range $5-7\times10^{-4}$ emu/mol. This behaviour is comparable to that previously found also in the partially oxidised gold analogue $(n\mathrm{Bu_4N})_2[\mathrm{Au(dcbdt)_2}]_5$ where the susceptibility was smaller (ca. $3-4\times10^{-4}$ emu/mol) as well as the Curie tail (ca. 0.7% of $S = {}^1/_2$ spins).

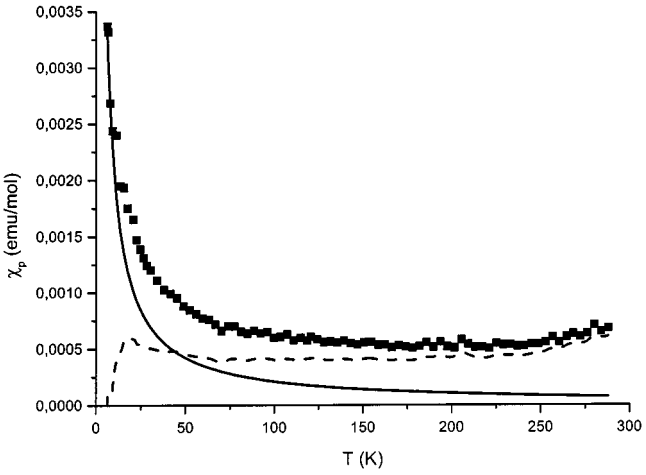

Figure 8. Paramagnetic susceptibility χ_p of $(n\mathrm{Bu_4N})_2[\mathrm{Ni(dcbdt)_2}]_5$ (**6**) as a function of the temperature T: the lines are a decomposition in a Curie tail, corresponding to ca. 5.6% of $S = {}^1/_2$ spins (full line) and the intrinsic susceptibility (− − −)

Although this behaviour of the paramagnetic susceptibility is reminiscent of a Pauli contribution, such a possibility is ruled out by the relatively low electrical resistivity as discussed below, and instead it should be seen as the result of complex antiferromagnetic interactions between the Ni^{III} states. The electrical conductivity, σ, of $(n\mathrm{Bu_4N})_2[\mathrm{Ni(dcbdt)_2}]_5$ (**6**), measured in single crystals is $\sigma_{rt} \approx 0.15$ S/cm at room temperature, following a thermally activated

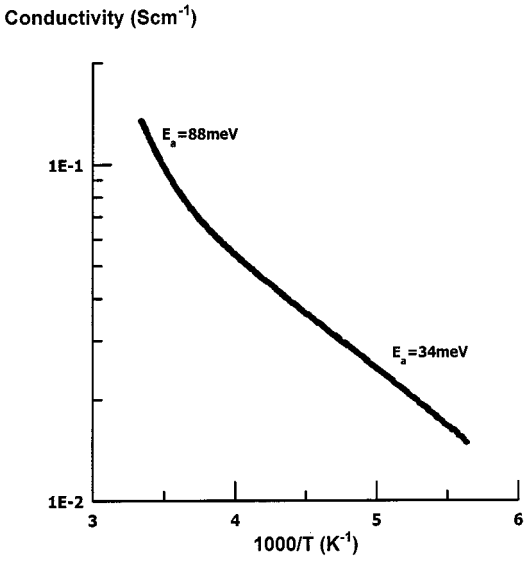

Figure 9. Electrical conductivity of $(n\mathrm{Bu_4N})_2[\mathrm{Ni(dcbdt)_2}]_5$ (**6**) single crystals as a function of the inverse temperature

semiconducting behaviour (Figure 9). The plot of logσ versus $1/T$ shows an activation energy of 88 meV at higher temperatures that decreases upon cooling, and was reduced to 34 meV below 250 K. This variation could be attributed to a change from an intrinsic to an extrinsic semiconducting regime upon cooling. The electrical conductivity of this compound was not as large as that of the gold analogue $(n\mathrm{Bu_4N})_2[\mathrm{Au(dcbdt)_2}]_5$, where the room-temperature value was $\sigma_{rt} \approx 11$ S/cm, with a smaller activation energy of 13.5 meV.[7] The thermoelectric power measurements in crystals of $(n\mathrm{Bu_4N})_2[\mathrm{Ni(dcbdt)_2}]_5$ indicated a value of $S_{rt} = -170$ μV/K at room temperature, also following a semiconducting behaviour with more negative values upon cooling in contrast to the gold analogue where the room-temperature thermopower value was rather small, $S_{rt} = -6$ μV/K, and slowly increased upon cooling, reaching a maximum of 20 μV/K at 120 K.[7] It was not possible to solve the crystal structure of $(n\mathrm{Bu_4N})_2[\mathrm{Ni(dcbdt)_2}]_5$ due to the poor diffracting quality of the crystals, and in the absence of the structure it was only possible to speculate about the reason for this difference in the electrical properties of the Ni and Au compounds. However, besides a possible stacking of the $\mathrm{Ni(dcbdt)_2}$ units in a more irregular way than in the Au analogue, but in a similar structure, the smaller conductivity and the larger activation energy observed in the Ni compound most probably reflects the different band filling.

Conclusion

In summary, we synthesized a new aromatic *ortho*-arenedithiol, which allowed the preparation of a new bis(dithiolate)nickel complex, that could exist in a broad range of oxidation states, dianionic, monoanionic, or mixed between monoanionic and neutral. The monoanionic complex presents a dimerisation of the $\mathrm{Ni(dcbdt)_2}$ units, the strongest found so far in an $\mathrm{Ni^{III}}$ complex. The partially oxidised compound $(n\mathrm{Bu_4N})_2[\mathrm{Ni(dcbdt)_2}]_5$ behaves as a semiconductor. This new dcbdt ligand opens the way for the preparation of a new family of transition metal complexes with other metallic elements such as Au, Pt, Pd, Cu, Co, and Fe. The use of the nickel complex as an electron acceptor in the preparation of different new charge-transfer salts is presently under way.

Experimental Section

General: Elemental analyses were performed by the analytical services of IST and ITN. − ^{1}H and ^{13}C NMR: Varian (300 MHz), [D$_6$]DMSO as solvent, TMS as internal standard. − IR: Perkin-Elmer 1330. − UV/Vis/NIR: Cary 5G Varian spectrophotometer. − MS: Fourier Transform Ion Cyclotron Resonance apparatus (EXTREL FTMS 2001) operated with a YAG laser source. − 4,5-Dichloro-1,2-dicyanobenzene was synthesized by literature methods.[8] DMF, acetonitrile, and dichloromethane were distilled from phosphorus pentoxide, while benzene was distilled from sodium. All other reagents were used without purification.

Synthesis of 1,2-Bis(*S*-benzylthio)-4,5-dicyanobenzene (2): To a suspension of sodium hydride (1.2 g, 51 mmol) in dry DMF (80 mL), phenylmethanethiol (6 ml, 51 mmol) was added under argon while keeping the temperature between 10 and 15 °C. At room temperature, **1** (5 g, 25 mmol) (Aldrich, TCI) was then added in small portions. The reaction mixture was left overnight under argon with stirring. The product was collected by filtration and recrystallized from $CHCl_3$/MeOH to give **2** as pale yellow needles. Yield 71%, m.p. 189−190 °C. − $C_{22}H_{16}N_2S_2$ (372.50): calcd. C 70.94, H 4.34, N 7.52, S 17.21; found C 70.28, H 4.44, N 7.42, S 16.91. − IR (KBr): $\tilde{\nu}$ = 3080 cm^{-1}, 2220, 1560, 1490, 1455, 1340, 1235, 1110. − ^{1}H NMR (CD_2Cl_2): δ = 7.47 (s, 2 H), 7.34 (m, 10 H), 4.24 (s, 4 H). − ^{13}C NMR (CD_2Cl_2): δ = 144.2, 135.0, 130.4, 129.3, 128.4, 115.8, 112.2, 37.9. − MS (EI, 70 eV): *m*/*z* (%) = 372 (13) [M$^+$], 281 (15), 203 (25), 91 (100), 83 (58).

Synthesis of 4,5-Dicyanobenzene-1,2-dithiol (3): A solution of **2** (3.0 g, 8.05 mmol) in dry benzene (100 mL) was added dropwise to a suspension of finely powdered anhydrous $AlCl_3$ (4.3 g, 32.2 mmol) in dry benzene (50 mL) and the mixture was stirred under argon at room temperature for 96 h. Ice/water was added (120 mL) and the organic layer was separated and washed successively with water and 5% aq. NaOH (3 × 80 mL). Upon acidification with 5% aq. HCl a yellowish solid precipitated that was filtered to give **3**. Yield 53%, m.p. 100 °C (dec.). − $C_8H_4N_2S_2$ (192.25): calcd. C 49.97, H 2.10, N 14.57, S 33.36; found C 50.78, H 2.02, N 13.93, S 32.76. − IR (KBr): $\tilde{\nu}$ = 3080 cm^{-1}, 2540, 2230, 1570, 1460, 1340, 1220. − ^{1}H NMR ([D$_6$]acetone): δ = 8.05 (s, 2 H), 3.84 (s, 2 H). − ^{13}C NMR ([D$_6$]acetone): δ = 141.0, 134.0, 116.1, 112.3.

Synthesis of $(n\mathrm{Bu_4N})_2[\mathrm{Ni(dcbdt)_2}]$ (4): Compound **3** (0.2 g, 1.04 mmol) was dissolved in 5 mL of NaOH aq. (5%). A solution of $n\mathrm{Bu_4NBr}$ (0.34 g, 1.05 mmol) in EtOH/H_2O (1:1) (5 mL) was added, followed by a solution of $NiCl_2{\cdot}6H_2O$ (0.12 g, 0.5 mmol) in the same solvent. The mixture was cooled and filtered, and the precipitate was washed with EtOH. The crude material was recrystallized from EtOH to give **4** as red needles. Yield 17%, m.p. 261−262 °C. − $C_{48}H_{76}N_6NiS_4$ (924.11): calcd. C 62.37, H 8.30, N 9.09, S 13.88; found C 62.38, H 8.28, N 8.92, S 13.62. − UV/Vis (CH_2Cl_2): λ (ε [Mcm^{-1}]) = 251.9 (31800), 281.6 (50700), 319.8 (52200), 406.0 (28700). − IR (KBr): $\tilde{\nu}$ = 3060 cm^{-1}, 2960−2860,

2220, 1530, 350. − ^{1}H NMR ([D$_6$]DMSO): δ = 7.24 (s, 4 H), 3.19 (t, 16 H, *J* = 8.5, *J* = 8.5), 1.57 (m, 16 H), 1.31 (m, 16 H), 0.93 (t, 24H *J* = 7.2, *J* = 7.2). − ^{13}C NMR ([D$_6$]DMSO): δ = 128.7, 120.8, 118.0, 101.6, 57.5, 23.0, 19.1, 13.4.

Synthesis of (nBu$_4$N)$_2$[Ni(dcbdt)$_2$]$_2$ (5): To a solution of **4** (0.17 g, 0.18 mmol) in acetone (100 mL) was added a solution of I_2 (70.1 mg, 0.28 mmol) in 5 ml of the same solvent. EtOH was added and the solution was slowly concentrated to give **5** as dark green needles. Yield 44%, m.p. 244−245 °C. − $C_{64}H_{80}N_{10}Ni_2S_8$ (1363.28): calcd. C 56.35, H 5.93, N 10.28, S 18.83; found C 55.85, H 6.03, N 10.13, S 18.39. − UV/Vis (CH_2Cl_2): λ (ε [mcm]) = 274.5 (7400), 319.8 (6000), 352.3 (4900), 854.3 (1400). − IR (KBr): $\tilde{\nu}$ = 3070 cm^{-1}, 2970, 2220, 1530, 420. − ^{1}H NMR ([D$_6$]acetone): δ = 7.98 (s, 4 H), 3.44 (t, 8 H, *J* = 7.8, *J* = 7.8), 1.85 (m, 8 H), 1.46 (m, 8 H), 0.99 (t, 12 H, *J* = 7.1, *J* = 7.1). − ^{13}C NMR ([D$_6$]acetone): δ = 135.5, 128.4, 123.9, 102.8, 47.1, 24.5, 20.5, 13.9. − MS: *m*/*z* (%) = 437.86 (100), 438.89 (14.9), 439.87 (48.83), 440.89 (9.49) 441.88 (10.63) 442.90 (1.82), 443.91 (2.02) [Ni(dcbdt)$_2^-$], 685.88 (4.33) 687.89(5.31) 689.89 (2.80) [Ni$_2$(dcbdt)$_3$]$^-$.

Synthesis of (nBu$_4$N)$_2$[Ni(dcbdt)$_2$]$_5$ (6): A solution of **5** (19.4 mg, 28.4 μmol) in dichloromethane (20 mL) was placed in a two-compartment electrocrystallisation cell, separated by a glass frit, with platinum electrodes. Employing galvanostatic conditions (ca. 1.5 μA/cm^2) for 5 d, dark brown thin needle-shaped crystals, with typical dimensions up to 2 × 0.1 × 0.05 mm, grew on the anode surface. The product was collected and washed with dichloromethane. M.p. > 240 °C. − $C_{112}H_{92}N_{22}Ni_5S_{20}$ (2680.81): calcd. C 50.18, H 3.46, N 11.49, S 23.92; found C 50.31, H 3.38, N 11.47, S 23.52.

Electrochemical Measurements: Cyclic voltammetry data were obtained using an EG&G Princeton Applied Research Electrochemical workstation. The measurements were performed at 20 °C in acetonitrile containing 0.1 M tetra-*n*-butylammonium perchlorate as supporting electrolyte with platinum working and counter-electrode and either a 0.1 M Ag/AgNO$_3$ or a calomel reference electrode and scan rates in the range 50−3000 mV s^{-1}.

X-ray Crystallographic Study: Data collection for both crystals of **4** and **5** was performed with an Enraf Nonius CAD4 diffractometer with graphite-monochromated Mo-K_α radiation (λ = 0.71069) at room temperature. Intensities were collected by the ω-2θ scan technique. The structures were solved by directed methods using SHELXS86[28] and refined with SHELXL97.[29] All non-hydrogen atoms were anisotropically refined by a full-matrix least-squares method. The hydrogen atoms were placed at calculated positions riding on the parent carbon atoms. Details of data collection and refinement are presented in Table 2. Molecular and crystal graphics were prepared with ORTEPIII[30] and SCHAKAL-97.[31] Crystallographic data (excluding structure factors) for the structures reported in this manuscript have been deposited with the Cambridge Crystallographic Data Centre. The deposition numbers are CCDC-154018 and -154019 for (nBu$_4$N)$_2$[Ni(dcbdt)$_2$] and (nBu$_4$N)[Ni(dcbdt)$_2$], respectively. Copies of the data can be obtained free of charge on application to CCDC, 12 Union Road, Cambridge CB2 1EZ, UK [Fax: (internat.) + 44-1223/336-033; E-mail: deposit@ccdc.cam.ac.uk].

EPR Measurements: EPR spectra in the range 4−300 K were obtained with an X-Band Bruker ESP 300E spectrometer equipped with a microwave bridge ER041XK, a rectangular cavity operating in T102 mode, a Bruker variable-temperature unit, an Oxford ESR-900 cryostat, and a field controller ER 032M system. The modulation amplitude was kept well below the line-width and the microwave power well below saturation.

Magnetic Susceptibility Measurements: Magnetic susceptibility measurements in the range 4−300 K were performed using a longitudinal Faraday system (Oxford Instruments) with a 7 T superconducting magnet under a magnetic field of 5 T and forward and reverse field gradients of 1 T/m. Polycrystalline samples (8−12 mg) were placed inside a previously calibrated thin-wall Teflon bucket. The force was measured with a microbalance (Sartorius S3D-V). Under these conditions the magnetisation was found to be proportional to the applied magnetic field.

Electrical Transport Measurements: Electrical conductivity and thermoelectric power measurements of selected single crystals were performed in the range 120−320 K, using a measurement cell attached to the cold stage of a closed-cycle helium refrigerator. In a first step, thermopower was measured using a slow AC (ca. 10^{-2} Hz) technique,[32] by attaching to the extremities of an elongated sample, with platinum paint (Demetron 308A), two 60 μm diameter 99.99% pure Au wires (Goodfellow Metals) thermally anchored to two quartz reservoirs, in a previously described apparatus,[33] operated by computer control.[34] In a second step, electrical resistivity measurements of the same sample were performed using a four-probe technique. Two extra Au wires were placed on the sample, in order to achieve a four-in-line contact configuration. Measurements were done imposing through the sample a current of 1 μA at low frequency (77 Hz) and measuring the voltage drop with a lock-in amplifier.

Acknowledgments

This work was partially supported by Fundação para a Ciência e Tecnologia (Portugal) under contracts PRAXIS XXI 2/2.1/QUI/203/94 and POCTI/1999/Qui/35452. H. A., D. B. and S. R. thank PRAXIS for their PhD grants. This work also benefited from COST action D14/0003/99.

[1] [1a] H. B. Gray, *Transition Met. Chem.* **1965**, *1*, 239−287. − [1b] G. N. Schrauzer, *Transition Met. Chem.* **1968**, *4*, 299−335. − [1c] J. A. McCleverty, *Prog. Inorg. Chem.* **1968**, *10*, 49. − [1d] D. Coucuvanis, *Prog. Inorg. Chem.* **1970**, *11*, 233. − [1e] R. Eisenberg, *Prog. Inorg. Chem.* **1970**, *12*, 295−369. − [1f] S. Alvarez, V. Ramon, R. Hoffman, *J. Am. Chem. Soc.* **1985**, *107*, 6253. − [1g] R. P. Burns, C. A. McAuliffe, *Adv. Inorg. Chem. Radiochem.* **1986**, *22*, 303−348.

[2] [2a] L. Alcácer, H. Novais, in *Extended Linear Chain Compounds*, vol. 3 (Ed.: J. S. Miller), Plenum Press, New York, **1983**, chapter 6, p. 319−351. − [2b] P. Cassoux, L. Valade, H. Kobayashi, A. Kobayashi, R. A. Clark, A. E. Underhill, *Coord. Chem. Rev.* **1991**, *110*, 115−160.

[3] G. Bähr, H. Schleitzer, *Chem. Ber.* **1955**, *88*, 1771.

[4] [4a] A. E. Hunderhill, M. M Ahmad, *J. Chem. Soc., Chem. Commun.* **1981**, 67−68. − [4b] A. Braude, K. Carneiro, C. S. Jacobsen, K. Mortensen, D. J. Turner, A. E. Underhill, *Phys. Rev. B.* **1987**, *35*, 7835. − [4c] A. E. Underhill, P. I. Clemenson, M. B. Hursthouse, R. L. Short, G. J. Ashwell, I. M. Sandy, K. Carneiro, *Synth. Met.* **1987**, *19*, 953−958.

[5] [5a] M. Almeida, R. T. Henriques, in *Handbook of Organic Conductive Molecules and Polymers* (Ed.: H. S. Nalwa), John Wiley and Sons, Chichester **1997**, vol. 1, chapter 2, p. 7. − [5b] V. Gama, R. T. Henriques, G. Bonfait, M. Almeida, S. Ravy, J. P. Pouget, L. Alcácer, *Mol. Cryst Liquid Cryst.* **1993**, *234*, 171−178.

[6] A. T. Coomber, D. Beljonne, R. H. Friend, J. L. Bredas, A. Charlton, N. Robertson, A. E. Underhill, M. Kurmoo, P. Day, *Nature* **1996**, *380*, 144.

[7] H. Alves, D. Simão, E. B. Lopes, D. Belo, V. Gama, M. T. Duarte, H. Novais, R. T. Henriques, M. Almeida, *Synth. Met.*, in press.

Table 2. Crystallographic data for $[Ni(dcbdt)_2]$ complexes

	$(nBu_4N)_2[Ni(dcbdt)_2]$	$(nBu_4N)_2[Ni(dcbdt)_2]_2$
Empirical formula	$C_{48}H_{76}N_6S_4Ni$	$C_{64}H_{80}N_{10}S_8Ni_2$
Crystal colour, habit	red, needle	green, needle
Molecular mass	924.1	681.64
Crystal system	monoclinic	triclinic
Space group	*C*2/*m*	$P\bar{1}$
Lattice constants [Å, °]	*a* =19.665(2)	*a* = 9.5061(10)
	b = 13.398(1)	*b* = 13.127(3)
	c = 9.758(1)	*c* = 16.045(3)
		α = 66.213(10)
	β = 94.16(1)	β = 85.715(10)
		γ = 70.363(10)
V [Å^3]	2564.2(4)	1721.2(5)
Z	2	1
ρ(calcd.) [Mg/m^3]	1.197	1.315
μ [mm^{-1}]	0.578	0.835
F(000)	996	718
θ range [°]	1.84−26.99.	1.78−26.97
Index ranges (*h*, *k*, *l*)	−25/25, −1/17, 12/1	−12/12, −16/15, −20/0
Reflections collected	3675	7712
Independent reflections	2881 [*R*int = 0.0439]	7441 [*R*int = 0.0547]
Data/parameters	2881/154	7441/398
Goodness-of-fit on F^2	0.965	1.054
Final *R* indices [$I > 2\sigma(I)$]	*R* = 0.0687	*R* = 0.0781
	*wR*2 = 0.0957	*wR*2 = 0.1088
Δρ: max./min. [e·Å^{-3}]	0.272/−0.297	0.248/−0.288

[8] D. Wöhrle, M. Eskes, K. Shigehara, A. Yamada, *Synthesis* **1993**, *32*, 3705.

[9] A. M. Richter, V. Engels, N. Beye, *Z. Chem.* **1989**, *29*, 444.

[10] D. E. L. Carrington, K. Clark, R. M. Scrowston, *J. Chem. Soc. C* **1971**, 3262.

[11] R. Williams, E. Billig, J. H. Waters, H. B. Gray, *J. Am. Chem. Soc.* **1966**, *88*, 43

[12] M. J. Baker-Hawkes, E. Billig, H. B. Gray, *J. Am. Chem. Soc.* **1966**, *88*, 4870−4875.

[13] N. C. Shiødt, P. Sommer Larsen, T. Bjørnholm, M. Folmer Nielsen, J. Larsen, K. Bechgaard, *Inorg. Chem.* **1995**, *34*, 3688−94.

[14] C. Mahadevan, M. Seshasayer, A. Radha, P. T. Manoharan, *Acta Crystallogr., Sect. C* **1984**, *40*, 2032.T. Yamamura, H. Arai, H. Kurihara, R. Kuroda, *Chem. Lett.* **1990**, 1975.

[15] E. Ribera, C. Rovira, J. Veciana, J. Tarrés, E. Canadell, R. Rousseau, E. Molins, M. Mas, J-P. Schoeffel, J.-P. Pouget, J. Morgado, R. T. Henriques, M. Almeida, *Chem. Eur. J.* **1999**, *5*, 2025.

[16] D. Sellmann, S. Funfgelder, F. Knoch, M. Moll, *Z. Naturforsch., Teil B* **1991**, *46*, 1601.

[17] J. V. Rodrigues, I. C. Santos, V. Gama, R. T. Henriques, J. C. Waerenborgh, M. T. Duarte, M. Almeida, *J. Chem. Soc., Dalton Trans.* **1994**, 2655−2660.

[18] [18a] W. C. Hamilton. I. Bernal, *Inorg. Chem.* **1967**, *6*, 2003. − [18b] A. L. Balch. I. G. Dance, R. H. Holm, *J. Am. Chem. Soc.* **1968**, *90*, 1139.

[19] H. Fujiwara, E. Ojima, H. Kobayashi, T. Courcet, I. Malfant, P. Cassoux, *Eur. J. Inorg. Chem.* **1998**, *11*, 1631−39.

[20] R.-M. Olk, R. Kirmse, E. Hoyer, C. Faulmann, P. Cassoux, *Z. Anorg. Alllg. Chem.* **1994**, *620*, 90.

[21] J. P. Cornelissen, J. G. Haasnoot, J. Reedijk, C. Faulmann, J.-P. Legros, P. Cassoux, P. J. Nigrey, *Inorg. Chim. Acta* **1992**, *202*, 131−139.

[22] J. Morgado, I. C. Santos, L. F. Veiros, R. T. Henriques, M. T. Duarte, M. Almeida, L. Alcácer, *J. Mat. Chem.* **1997**, *7*, 2387−2392.

[23] C. J. Firch Jr., *Acta Crystallogr.* **1966**, *20*, 107.

[24] A. Kobayashi, Y. Sasaki, *Bull. Chem. Soc. Jpn.* **1977**, *50*, 2650.

[25] V. Gama, I. C. Santos, G. Bonfait, R. T. Henriques, M. T. Duarte, J. C. Waerenborgh, L. Pereira, J. M. P. Cabral, M. Almeida, *Inorg. Chem.* **1992**, *31*, 2598−2604.

[26] R. L. Carlin, *Magnetochemistry*, Springer-Verlag, Berlin, **1986**.

[27] J. F. Veiher, L. R. Melby, R. E. Benson, *J. Am. Chem. Soc.* **1964**, *86*, 4329.

[28] *SHELXS86*: G. M. Sheldrick, *Acta Crystallogr., Sect. A* **1990**, *46*, 467−473.

[29] G. M. Sheldrick, *SHELXL97*, *A Program for Crystal structure refinement*, University of Göttingen, Germany, **1997**.

[30] M. N. Burnett, C. K. Johnson, *ORTEPIII*, Report ORNL-6895, Oak Ridge National Laboratory, Tennessee, USA, **1996**.

[31] E. Keller, *SCHAKAL-97*, *A Computer Program for the Representation of Molecular and Crystallographic Models*, Kristallographisches Institut der Universität Freiburg i. Br., Germany, **1997**.

[32] P. M. Chaikin, J. F. Kwak, *Rev. Sci. Instrum.* **1975**, *46*, 218.

[33] M. Almeida, S. Oostra, L. Alcácer, *Phys. Rev. B* **1984**, *30*, 2839−2845.

[34] E. B. Lopes, *INETI-Sacavém*, internal report, **1991**.

Received January 22, 2001
[I01029]